

## Free Energy and Entropy of Activation for Phospholipid Flip-Flop in Planar Supported Lipid Bilayers

Timothy C. Anglin, Michael P. Cooper, Hao Li, Katherine Chandler, and John C. Conboy\*

University of Utah Department of Chemistry, 315 South 1400 East, Salt Lake City, Utah 84112

Received: September 22, 2009; Revised Manuscript Received: December 9, 2009

Basic transition state theory is used to describe the activation thermodynamics for phospholipid flip-flop in planar-supported lipid bilayers (PSLBs) prepared by the Langmuir–Blodgett/Langmuir–Schaeffer method. The kinetics of 1,2-distearoyl-*sn*-glycero-3-phosphocholine (DSPC) flip-flop were determined as a function of temperature and lateral surface pressure using sum-frequency vibrational spectroscopy (SFVS). From the temperature and lateral pressure dependent DSPC flip-flop kinetics, a complete description of the activation thermodynamics for flip-flop in the gel state, including free energy of activation ( $\Delta G^\ddagger$ ), area of activation ( $\Delta a^\ddagger$ ), and entropy of activation ( $\Delta S^\ddagger$ ), was obtained. The free energy barrier for flip-flop of DSPC was determined to be  $\Delta G^\ddagger = 105 \pm 2$  kJ/mol at 40 °C at a deposition surface pressure of 30 mN/m. The free energy barrier was found to consist of large opposing entropic and enthalpic contributions. The influence of alkyl chain length on the activation thermodynamics of flip-flop was also investigated. Decreasing the alkyl chain length led to a decrease in  $\Delta G^\ddagger$  due primarily to an increase in  $\Delta S^\ddagger$ . The values obtained here are compared to previous studies investigating flip-flop by vesicle based methods.

### Introduction

The thermodynamic barrier to transmembrane diffusion of phospholipids (flip-flop) in cellular membranes has long interested researchers. It is generally accepted that a significant barrier to flip-flop exists which is related to the energetic penalty of moving the hydrophilic headgroup of a phospholipid through the hydrophobic core of the membrane.<sup>1,2</sup> Overcoming this energetic barrier represents the rate limiting step in the spontaneous flip-flop of phospholipids in biological membranes, yet, while numerous kinetic studies of phospholipid flip-flop have been conducted,<sup>3–10</sup> few researchers have reported thermodynamic parameters for the process.<sup>7–9</sup> The only examples to date which have explicitly treated the free energy dependence of flip-flop have relied on systems exhibiting both intervesicle exchange and transmembrane diffusion in liquid phase vesicles, where the calculated results depend on the model used to deconvolute the observed movement of probe molecules.<sup>7–9</sup> Regrettably, the direct measurement of native lipid flip-flop in solution phase vesicles is not currently possible. In contrast to vesicle based models for the study of flip-flop, planar-supported lipid bilayers (PSLBs) allow direct measurement of flip-flop in a single bilayer without requiring intervesicle exchange. In addition, PSLBs prepared by the Langmuir–Blodgett (LB)/Langmuir–Schaeffer (LS) method allow for accurate control of lipid packing density which facilitates a more detailed thermodynamic analysis of lipid translocation. PSLBs are also quite amenable to study by sum-frequency vibrational spectroscopy (SFVS). SFVS can be used to track the movement of phospholipids in a PSLB without requiring the use of chemically modified (fluorescent- or spin-labeled) lipid molecules, providing a distinct advantage over previous methods. We discuss herein the measurement of phospholipid flip-flop in pure phospholipid bilayers as a function of both lateral pressure and temperature in the membrane, allowing for the determination of the

underlying activation thermodynamics for this important biophysical process. This approach also allows us to elucidate the role lateral pressure plays in governing the energetics of lipid flip-flop and to independently measure the various components (work, entropy, enthalpy) of the free energy of activation.

**Biological Significance of Flip-Flop.** It is widely known that lipid flip-flop has an important role in the regulation of cell growth and intercellular signaling.<sup>1,11,12</sup> Thus, the study of lipid flip-flop kinetics has attracted the interest of researchers for many years, and a wide variety of techniques including fluorescence, NMR, electron spin resonance (ESR), and small angle neutron scattering have been employed to measure lipid flip-flop, primarily in solution phase vesicles.<sup>3,6,7,10,12–14</sup> Additional studies have made use of phospholipase assays or bovine serum albumin (BSA) extraction of lipids in order to determine the rate of lipid flip-flop in biologically relevant membranes.<sup>15,16</sup> There have also been attempts to model flip-flop computationally.<sup>17–21</sup> Given the time scale involved, this approach is generally too computationally demanding for atomistic scale modeling of a large number of lipids and vastly simplified models (coarse-grain) are instead used.<sup>18,19</sup> Alternatively, detailed modeling can be performed for cases in which a stimulus for lipid flip-flop is provided in order to decrease the calculation time needed to observe the event.<sup>17,21</sup> However, it is unclear whether the application of such a stimulus is justified. In spite of the general interest, there are only a handful of publications which report measured thermodynamic parameters for lipid flip-flop, most of which utilize chemically modified probes or which rely on intervesicular exchange.<sup>5–7,22,23</sup>

It is concerning to note that much of our understanding of lipid flip-flop has been obtained from lipid probe molecules which may not represent the true behavior of the native lipid species. Among those studies mentioned above, there has only been one attempt to determine the free energy of activation for phospholipid flip-flop of a chemically unmodified lipid.<sup>7</sup> This is surprising when one considers the importance of the energy barrier to phospholipid flip-flop in the maintenance of phos-

\* To whom correspondence should be addressed. E-mail: conboy@chem.utah.edu. Telephone: (801) 585-7957. Fax: (801) 581-8433.

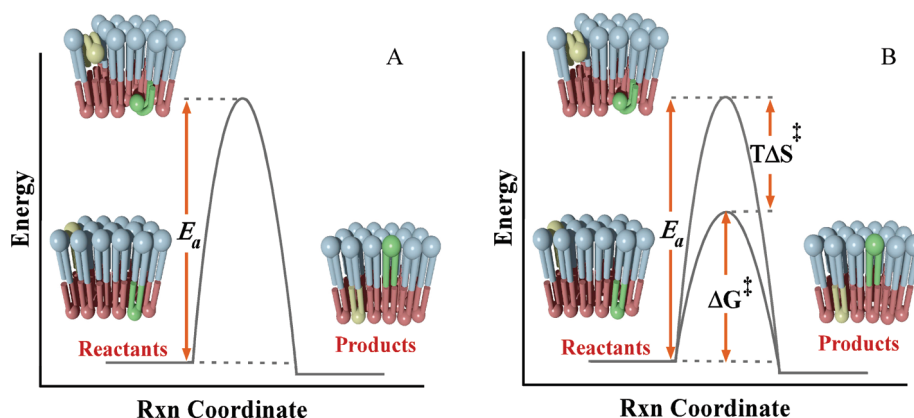


**Figure 1.** Reaction coordinate diagrams for the process of phospholipid flip-flop: panel (A) illustrates the reaction coordinate diagram for flip-flop according to Arrhenius theory, where the Arrhenius activation energy is considered to be primarily enthalpic; panel (B) illustrates the corresponding diagram for flip-flop according to transition state theory, where the energy barrier is instead shown as the free energy of activation. The Arrhenius approach neglects the entropic contribution and therefore overestimates the total free energy barrier. In both cases, the process of flip-flop is illustrated for individual lipids in each leaflet. The molecules begin in an ordered ground state, proceed through an energetically unfavorable transition state, and end in an ordered final state in the opposite leaflet. The illustration is not meant to indicate cooperativity of flip-flop across the bilayer.

pholipid asymmetry in cellular membranes.<sup>24–27</sup> It is therefore of the utmost importance to acquire a detailed description of the activation thermodynamics and transition state for phospholipid flip-flop in order to more fully elucidate the quintessential process of lipid translocation.

Recent work in our laboratory has demonstrated the use of SFVS to measure flip-flop kinetics of native phospholipids without the need for chemical modification.<sup>5,22,28</sup> The temperature dependence for this process was examined and modeled by Arrhenius theory in order to derive an Arrhenius activation energy ( $E_a$ ) of  $206 \pm 18$  kJ/mol for flip-flop of DSPC in the gel phase.<sup>5</sup> The large Arrhenius activation energy was balanced by an anomalously large Arrhenius pre-exponential factor  $A$  of  $3.6 \times 10^{29} \text{ s}^{-1} \pm 3.7 \times 10^{28} \text{ s}^{-1}$ . Typical values for  $A$  range from  $10^{10}$  to  $10^{16} \text{ s}^{-1}$  for most chemical reactions, with  $A$  representing the collision/fragmentation frequency resulting in product formation.<sup>29</sup> For the case of lipid flip-flop,  $A$  represents the frequency of successful attempts to cross the bilayer.<sup>5</sup> The range of  $A$  is typically found to fall within the frequencies of molecular motions or molecular vibrations which lead to product formation; thus, the occurrence of anomalously high pre-exponential values is concerning, as it would lead to a nonsensical physical interpretation. However, this analysis may be complicated when strong thermodynamic contributions from entropy exist.<sup>29</sup> The process of phospholipid flip-flop is just such a case. Phospholipid flip-flop can be viewed as an entropy driven diffusive process wherein the Brownian motion of the molecules in the bilayer is responsible for their transport across the bilayer.<sup>6,17,23</sup> As such, any thermodynamic description of flip-flop must describe the role of entropy in the process of interbilayer lipid exchange.

Thermodynamic analysis according to Arrhenius theory generally neglects entropic contributions and assumes that  $E_a$  and  $A$  are independent of, or only weakly dependent on, temperature.<sup>30</sup> The surprisingly large value of  $A$  measured for DSPC flip-flop is likely indicative of a large entropic contribution to the process, as the entropic effect would be manifest in the Arrhenius pre-exponential factor ( $A$ ).<sup>29</sup> Given the likelihood of an entropic driving force, one approach is to model phospholipid flip-flop in the more general framework of transition state theory (TST), which explicitly treats the entropic contribution to the activation thermodynamics and can be easily related to the Arrhenius treatment. In this work, we will demonstrate the application of TST to study the activation free

energy ( $\Delta G^\ddagger$ ) and activation entropy ( $\Delta S^\ddagger$ ) for flip-flop of native (unlabeled) phospholipids in PSLBs. A brief introduction and comparison of the Arrhenius and TST thermodynamic approaches is provided before the results and analysis are presented.

## Theory

**Arrhenius Kinetic Theory.** The Arrhenius equation describes the rate of a reaction according to eq 1 where  $k$  is the rate of reaction,  $A$  is the pre-exponential factor,  $E_a$  is the activation energy,  $R$  is the ideal gas constant, and  $T$  is the temperature.

$$k = A e^{-E_a/RT} \quad (1)$$

This empirical relationship is often used to characterize the dependence of a reaction rate on temperature and derive the thermodynamic parameters  $E_a$  and  $A$  from known rates and temperatures. As discussed above,  $E_a$  represents an activation barrier for the reaction which is primarily enthalpic in nature, and  $A$  is interpreted as being related to the frequency of successful events leading to product formation.<sup>30</sup> The potential energy surface shown in Figure 1A is specific to the Arrhenius treatment due to its dependence on enthalpy and  $E_a$ , as expressed by

$$E_a = \Delta H^\ddagger - P\Delta V^\ddagger + RT \quad (2)$$

where  $\Delta H^\ddagger$  is the enthalpy of activation,  $\Delta V^\ddagger$  is the activation volume, and  $P$  is pressure.<sup>30</sup> In most cases, the pressure dependent term is small and  $E_a$  is often treated as a purely enthalpic barrier ( $E_a \approx \Delta H^\ddagger$ ). Arrhenius theory is sufficiently general to allow modeling of phospholipid flip-flop thermodynamics, as it can be applied to any kinetic process which demonstrates an exponential dependence on temperature. However, the contribution to the energy barrier due to entropy is difficult to interpret by this method, as the entropic contribution is manifest in  $A$ . Therefore, Arrhenius analysis of lipid flip-flop provides an incomplete thermodynamic picture, as it does not explicitly treat the entropic contribution and leads to a nonsensical interpretation of the pre-exponential factor  $A$ . It is often more convenient to conceptualize the thermodynamics of a reaction according to the free energy, enthalpy, and entropy

rather than frequency factor and Arrhenius activation energy. This is done by application of transition state theory.

**Transition State Theory.** A complete review of transition state theory will not be provided here, but it may be found elsewhere.<sup>30–33</sup> This treatment will outline only the salient aspects of the theory. Figure 1B shows a general potential energy surface for a reaction according to TST. This is notably different from Figure 1A in the dependence of the reaction on the free energy of activation ( $\Delta G^\ddagger$ ), rather than a purely enthalpic term. The total barrier, given by  $\Delta G^\ddagger$ , reflects both enthalpic and entropic contributions and leads to a more straightforward interpretation of the energetic barrier for processes in which entropy is non-negligible.

The rate of reaction as a function of temperature according to TST is given as

$$k = \frac{k_B T}{h} e^{(-\Delta G^\ddagger/RT)} \quad (3)$$

where  $\Delta G^\ddagger$  is the free energy of activation,  $k_B$  is Boltzman's constant,  $h$  is Plank's constant, and  $T$  is the temperature.<sup>30,31</sup> The free energy of activation for the specific case of lipid flip-flop may be expressed as

$$\Delta G^\ddagger = E_a - RT + \Pi \Delta a^\ddagger - T \Delta S^\ddagger \quad (4)$$

where  $\Delta S^\ddagger$  is the entropy of activation and  $\Pi \Delta a^\ddagger$  is a two-dimensional work term (analogous to  $P \Delta V^\ddagger$ ) depending upon the lateral surface pressure ( $\Pi$ ) and an area of activation ( $\Delta a^\ddagger$ ). The use of a two-dimensional work term arises from the description of the lipid bilayer system as a two-dimensional gas whose pressure dependence is better described by a lateral surface pressure ( $\Pi$ ) rather than  $P$ .<sup>34,35</sup> Reduction of the pressure term to the corresponding two-dimensional analogs yields an expression which depends on an area of activation ( $\Delta a^\ddagger$ ) rather than an activation volume. The activation area for phospholipid flip-flop represents the change in area occupied by a lipid in the bilayer upon going from the ground state to the flip-flop transition state, and it is indicative of the per molecule local expansion of the bilayer that must occur in order to accommodate transfer of a phospholipid across the bilayer. Further details may be found in our previous work, wherein we reported our findings on the experimental determination of  $\Delta a^\ddagger$  for flip-flop of 1,2-dipalmitoyl-*sn*-glycero-3-phosphocholine (DPPC).<sup>36</sup>

Equation 4 allows for explicit determination of the lateral pressure dependence of, and entropic contributions to, the energy barrier for the reaction. Equation 4 may be substituted into the rate expression to yield eq 5, which describes the dependence of the rate of reaction on the Arrhenius activation energy, the activation entropy, and the work required to reach the transition state.

$$k = \frac{k_B T}{h} e^{((-E_a/RT) - (\Pi \Delta a^\ddagger/RT) + (T \Delta S^\ddagger/RT) + 1)} \quad (5)$$

It is possible to relate the rate expression given above to that found in Arrhenius rate theory by a simple rearrangement of terms. The rate expressions according to TST and Arrhenius rate theory are presented on the left and right-hand sides of eq 6, respectively:

$$k = \frac{k_B T}{h} e^{(1 - (\Pi \Delta a^\ddagger/RT) + (T \Delta S^\ddagger/RT))} e^{(-E_a/RT)} = A e^{(-E_a/RT)} \quad (6)$$

Relating the Arrhenius pre-exponential factor to the leading terms in the TST rate expression gives

$$A = \left( \frac{k_B T}{h} \right) e^{(1 - (\Pi \Delta a^\ddagger/RT) + (\Delta S^\ddagger/R))} \quad (7)$$

Equation 7 clearly shows the dependence of  $A$  on the entropy of activation and temperature for the reaction, as well as the area of activation and surface pressure for the lipid membrane. This equation may be rearranged and solved for the activation entropy for phospholipid flip-flop:

$$\Delta S^\ddagger = R \left( \ln \left( \frac{Ah}{k_B T} \right) + \left( \frac{\Pi \Delta a^\ddagger}{RT} \right) - 1 \right) \quad (8)$$

The activation entropy for flip-flop may thus be determined if both the lateral pressure dependence and temperature dependence of the rate for the system is known. This requires two separate studies to determine the temperature dependence at fixed pressures, and the investigation of the pressure dependence of the lipid flip-flop rate as fixed temperatures. Using the lateral pressure and temperature dependent rate data, it is possible to calculate not only the Arrhenius parameters but also the area of activation, entropy of activation, and ultimately the free energy of activation for phospholipid flip-flop. Thus, a complete description of the activation thermodynamics for phospholipid flip-flop is possible.

The relationship between the inward and outward flipping of lipids should also be considered. An essential assumption of TST is that molecules reaching the transition state will proceed to products without recrossing the transition state.<sup>30,32</sup> Given the symmetry of the phospholipid bilayer, and the requirement that mass is conserved between the two bilayer leaflets, phospholipids which cross from one leaflet to the other must be balanced eventually by transfer of a phospholipid in the opposite direction. The forward and reverse flipping of phospholipids in the laboratory frame should not be confused as a thermodynamic recrossing of the transition state. The model employed in our analysis does not distinguish a ground state molecule in one leaflet from an equivalent ground state in the opposite leaflet. The symmetry of the bilayer is such that the thermodynamics for movement in each direction are equal.<sup>5</sup> Instead, the flipping of a phospholipid from one leaflet to the other is governed by the same reaction coordinate diagram, which is symmetric with respect to the coordinate of the bilayer normal, about the center of the bilayer. The return of a phospholipid to its original leaflet after first undergoing a "flip" event to reach the opposite side will affect the observed SFVS signal, yet this effect has been accounted for in the kinetic expression used to fit the observed signal decay, which is discussed below.<sup>5</sup>

Transition state theory has been previously applied to the study of lipid flip-flop by investigating the temperature dependence of the rate of lipid flip-flop, as calculated from intervesicle exchange studies.<sup>7,9,37</sup> In addition, Homan and Pownall have studied the influence of applied external pressure on the exchange and flip-flop of (1-octanoyl-2-[9-(1-pyrenyl)nonanoyl]-phosphatidylethanolamine (OPNPE)) in vesicles over a range



of 1 bar to several kbar.<sup>23</sup> To our knowledge, their study is the only one to date which has studied the effect of applied pressure on the kinetics of flip-flop. Given the two-dimensional nature of the lipid bilayer membrane, very large applied pressures are necessary to induce small differences in the lateral pressure and packing density in solution phase vesicles. The authors noted that the minor changes in packing density ( $\sim 4\%$ ) over the large applied pressure range were most likely responsible for the change in kinetics of transmembrane probe transfer.<sup>23</sup> The approach of Homan and Pownall illustrates the modulating effect of pressure on the kinetics of lipid flip-flop. However, these studies were still dependent on the use of chemically modified probe molecules. The results of this approach are also more difficult to interpret, due to the difficulty of deconvoluting the effects of changing lipid packing density and bilayer thickness. Ideally, one would like to control the lateral pressure and packing in the membrane without the requirement of large external pressures or concomitant alteration of the bilayer thickness. In our current approach, the lipid bilayer membranes are treated as two-dimensional rather than three-dimensional thermodynamic systems, consistent with previous experimental and theoretical efforts.<sup>38,39</sup> Although either approach is valid, the experimental methods and interpretation are greatly simplified in the two-dimensional case. The direct control of packing density and lateral surface pressure by the LB/LS method of bilayer formation provides a more direct analysis of the effect of packing on the rate of flip-flop without the need to apply large external pressures. By studying the influence of lateral pressure on the thermodynamics of native lipids in a single PSLB, we hope to provide a complete and accurate description of flip-flop for an unmodified lipid species.

**Measurement of Phospholipid Flip-Flop Kinetics by SFVS.** The kinetics of phospholipid flip-flop in planar supported lipid bilayers can be readily studied using sum-frequency vibrational spectroscopy (SFVS).<sup>5,22</sup> SFVS is finding an increasing number of applications for the study of biological interfacial phenomena.<sup>40–44</sup> This is due to the ability of SFVS to probe interfacial molecules in a surface-specific manner without the need for chemical modification. The surface specificity of SFVS is a consequence of the symmetry constraints for the nonlinear optical process, where the sum-frequency signal may be produced only at an interface or in media that lack inversion symmetry and no signal is produced in the bulk of an isotropic media.<sup>45,46</sup> This is used to great advantage in the study of phospholipid flip-flop, where the ability to measure the behavior of native lipid species is essential. Our laboratory has previously shown that the headgroup modification of a lipid with a TEMPO spin-label probe can significantly alter flip-flop kinetics.<sup>5</sup> The ability to directly detect native lipid species is essential to an accurate measurement of lipid flip-flop kinetics and thermodynamics. Further discussion of the specific application of SFVS to the study of lipid flip-flop may be found in earlier publications.<sup>5,22,47</sup>

Experimentally, SFVS involves overlapping, both spatially and temporally, a fixed frequency visible ( $\omega_{\text{vis}}$ ) and tunable infrared laser source ( $\omega_{\text{IR}}$ ) at an interface, where photons at the sum of the input beam frequencies are produced, expressed as

$$\omega_{\text{Sum}} = \omega_{\text{vis}} + \omega_{\text{IR}} \quad (9)$$

The intensity of the light generated at  $\omega_{\text{Sum}}$  depends on the square of the Fresnel coefficients for the sum-frequency ( $\tilde{f}_{\text{SF}}$ ), visible ( $f_{\text{vis}}$ ), and infrared beams ( $f_{\text{IR}}$ ) which describe the magnitude of the electric field at the interface for a given

polarization and incident angle of the fundamental fields, as well as the second-order nonlinear susceptibility tensor ( $\chi^{(2)}$ ) which describes the response of the molecules comprising the interface to the input electric fields (eq 10).<sup>48,49</sup>

$$I_{\text{SFVS}} = \left| \tilde{f}_{\text{SF}} f_{\text{vis}} f_{\text{IR}} \chi^{(2)} \right|^2 \quad (10)$$

The susceptibility tensor  $\chi^{(2)}$  may be expressed in terms of a resonant  $\chi_{\text{R}}^{(2)}$  and nonresonant contribution  $\chi_{\text{NR}}^{(2)}$  by the following expression:

$$\chi^{(2)} = \chi_{\text{R}}^{(2)} + \chi_{\text{NR}}^{(2)} \quad (11)$$

The resonant contribution  $\chi_{\text{R}}^{(2)}$  may be further expanded in terms of the IR ( $A_i$ ) and Raman transition probabilities ( $M_{jk}$ ), where  $N$  is the number of molecules at the interface,  $\omega_v$  is the frequency of the  $v$ th normal mode vibration,  $\omega_{\text{IR}}$  is the IR input frequency, and  $\Gamma_v$  is the line width of the  $v$ th transition:

$$\chi_{\text{R}}^{(2)} = \sum_v \frac{N \langle A_i M_{jk} \rangle}{\omega_v - \omega_{\text{IR}} - i\Gamma_v} \quad (12)$$

The brackets ( $\langle \rangle$ ) in eq 12 denote an ensemble orientational average for the transition dipoles at the interface. A SFVS spectrum is obtained by scanning the input IR frequency, where an enhancement in SFVS signal will be found when the IR frequency corresponds to a normal mode vibration of the molecules at the interface.

Within a phospholipid bilayer, the relative orientation of lipids comprising the proximal and distal leaflets will also influence the observed SFVS signal, as transitions with opposite orientation within the bilayer will interfere destructively due to the coherent nature of SFVS. This can be illustrated by considering the symmetric stretching vibration of the terminal methyl group ( $\text{CH}_3 \nu_s$ ) on each phospholipid alkyl chain, with the methyl groups in each leaflet having a transition with opposite orientation along the surface normal.<sup>47</sup> In this orientation ( $\text{CH}_3 \nu_s$ ) transitions excited in the upper leaflet will have opposite phase relative to those in the lower leaflet, leading to destructive interference (see inset, Figure 2).

If the lipid molecules comprising both leaflets of the bilayer are the same species, there will be complete cancellation of the SFVS contributions from each leaflet and no net signal will be observed. However, if the bilayer is prepared such that perdeuterated lipids occupy one leaflet opposite a leaflet of their proteated analogues, then  $\chi_{\text{R}}^{(2)}$  will be nonzero, as the transition dipole of the perdeuterated species lies at lower frequency and cannot interfere with the SFVS response of the proteated lipid molecules. For such a system, the SFVS signal intensity (arising from the lipid species) is directly related to the degree of asymmetry in the distribution of proteated and perdeuterated lipid species within the bilayer. (This is illustrated in Figure 2 (blue), which shows the SFVS spectrum of an asymmetric bilayer of DSPC (LB layer) and DSPC- $d_{70}$  (LS layer).) The asymmetric bilayer experiences no cancellation between the upper and lower leaflets, providing ample SFVS signal. However, a symmetric bilayer consisting of 1:1 DSPC:DSPC- $d_{70}$  in both leaflets experiences complete cancellation between the upper and lower leaflets, and no vibrational resonances are visible in the SFVS spectrum (Figure 2, black). The low signal observed in the symmetric case demonstrates the dipole cancel-

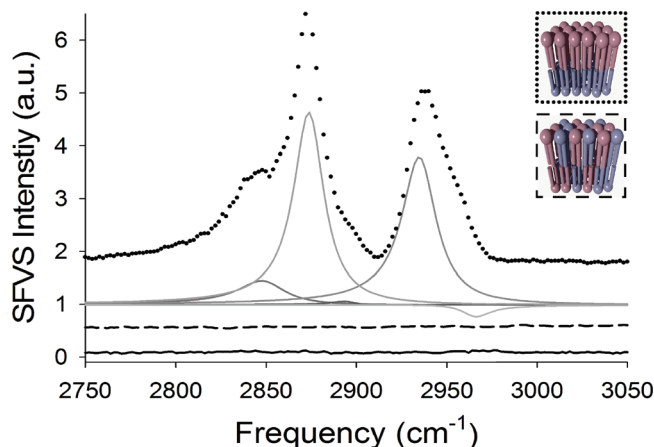


**Figure 2.** SFVS spectrum of an asymmetric DSPC/DSPC- $d_{70}$  bilayer at room temperature (data points shown in black). The individual vibrational contributions, as determined by fitting the data to eq 12 (gray), are also shown in gray. The observed peaks correspond to the  $\text{CH}_2$  symmetric stretch ( $\nu_s$ ) at  $2848\text{ cm}^{-1}$ , the  $\text{CH}_3$  ( $\nu_s$ ) at  $2875\text{ cm}^{-1}$ , the  $\text{CH}_2$  Fermi resonance (FR) at  $2905\text{ cm}^{-1}$ , the  $\text{CH}_3$  FR at  $2938\text{ cm}^{-1}$ , and the  $\text{CH}_3$  antisymmetric stretch ( $\nu_{as}$ ) at  $2967\text{ cm}^{-1}$ . The sample was then held at  $46.8\text{ }^\circ\text{C}$  until the SFVS signal reached a minimum following flip-flop of the sample. A spectrum was again obtained after the sample was returned to room temperature (dashed line). For comparison, a symmetric bilayer consisting of a 1:1 ratio of DSPC and DSPC- $d_{70}$  was prepared and a spectrum obtained at room temperature (solid black line). The spectra are offset for clarity. Inset: Illustrations of an asymmetric (black dots) and symmetric bilayers (dashed line).

lation from similar species in opposite leaflets and typifies the SFVS spectrum observed from symmetric gel phase bilayers.

Phospholipid flip-flop may be followed for an initially asymmetric PSLB by observing the decay in SFVS signal as lipid flip-flop proceeds and the system becomes more symmetric. The SFVS intensity may thus be related to the bilayer asymmetry in a time dependent manner.<sup>22</sup> The rate expression which describes the decay in the SFVS intensity due to lipid exchange is given by<sup>5,22</sup>

$$I_{\text{CH}_3}(t) = I_{\text{max}} e^{(-4kt)} + I_0 \quad (13)$$

where  $I_{\text{CH}_3}(t)$  is the time dependent SFVS signal observed for the  $\text{CH}_3$   $\nu_s$  vibrational mode at  $2875\text{ cm}^{-1}$ ,  $I_{\text{max}}$  is initial maximum signal at the start of the decay ( $t = 0$ ),  $k$  is the rate constant for flip-flop, and  $I_0$  is the baseline offset to the data due to any nonresonant SFVS signal and instrument offset. A full derivation of the rate expression is given elsewhere.<sup>5,22</sup> The rate constant  $k$  for phospholipid flip-flop may be determined by fitting the observed change in SFVS intensity to eq 13.

## Materials and Methods

1,2-Distearoyl-*sn*-glycero-3-phosphocholine (DSPC), 1,2-distearoyl-D70-*sn*-glycero-3-phosphocholine (DSPC- $d_{70}$ ) (DPPC), 1,2-dipalmitoyl-D62-*sn*-glycero-3-phosphocholine (DPPC- $d_{62}$ ), 1,2-dimyristoyl-*sn*-glycero-3-phosphocholine (DMPC), and 1,2-dimyristoyl-D54-*sn*-glycero-3-phosphocholine (DMPC- $d_{54}$ ) were purchased from Avanti Polar Lipids (Alabaster, AL). Spectrometric grade chloroform was purchased from Mallinckrodt Baker Bioscience (Phillipsburg, NJ). Hemicylindrical fused silica prisms were purchased from Almaz Optics (Marlton, NJ). All water used in this study was purified by using a Nanopure Infinity purification system (Barnstead Thermolyne) to a minimum resistivity of  $18.2\text{ M}\Omega\cdot\text{cm}$ .

Phospholipid solutions were prepared in chloroform at a concentration of  $1\text{ mg/mL}$ . Individual lipid solutions were spread at the air–water interface of a KSV Instruments minitrough (Helsinki, Finland), and the solvent was allowed to evaporate until a stable surface pressure reading was obtained. The monolayers were then compressed to the desired surface pressure and deposited onto a fused silica prism substrate by controlled withdrawal of the prism from the subphase in a vertical orientation (LB transfer). The trough was then cleaned and a new lipid solution spread at the interface. After equilibration of the monolayer and subsequent compression to the desired surface pressure, the second leaflet was deposited by transfer of the prism from air into the subphase in a horizontal orientation (LS transfer). Following deposition, the sample is maintained in an aqueous environment during transfer to a custom flow cell and throughout the experiment. Prior to obtaining an SFVS spectrum, the cell is flushed with  $\text{D}_2\text{O}$  in order to avoid spectral interference. Temperature control for the bilayer sample was provided by means of a thermoelectric heating unit (TE Technologies, Traverse City, MI) incorporated into the Teflon sample cell. Further details of the sample deposition technique may be found elsewhere.<sup>47</sup>

SFVS experiments were conducted using a custom built OPO/OPA system from LaserVision (Bellevue, WA), which is pumped by a Continuum Surelite I NdYAG laser. In all cases, the input visible and IR beams were *s* and *p* polarized, respectively, resulting in an *s* polarized sum-frequency output. This polarization combination is employed in order to probe the vibrations along the surface normal. Additional details on the laser system and configuration of the SFVS spectrometer may be found elsewhere.<sup>5,22,47</sup>

SFVS spectra were obtained for each sample in order to verify membrane integrity. After obtaining a spectrum, the samples were subsequently heated to the desired temperature and maintained at elevated temperature for the duration of the experiment. Typically, the temperature of the cell reached a stable value between 300 and 500 s after initiating the temperature rise. The SFVS signal at  $2875\text{ cm}^{-1}$  was monitored continuously during this process with little signal change during the initial heating period. The decay in signal after reaching a stable temperature follows an exponential decay and was fit according to eq 13 in order to obtain the rate constant  $k$  for phospholipid flip-flop. In order to determine the dependence of  $k$  on  $\Pi$ , numerous samples were prepared at a common temperature ( $24\text{ }^\circ\text{C}$ ) over a range of varying deposition pressures. The rate of SFVS signal decay was then collected for each of these samples at a common elevated temperature ( $46.8\text{ }^\circ\text{C}$ , for instance). In this fashion, a set of data were produced which represent the pressure dependence of  $k$  at a single decay temperature ( $46.8\text{ }^\circ\text{C}$ ). Additional data sets were produced in this manner for 40, 42, 43, and  $50\text{ }^\circ\text{C}$  as well. In all cases, sample deposition pressures were the same in each leaflet of the deposition, although the pressure from sample to sample was varied.

## Results and Discussion

A representative SFVS spectrum of an asymmetric DSPC/DSPC- $d_{70}$  bilayer is shown in Figure 2 (black). The data were fit according to eq 12, with the individual peak fits shown in gray. The most prominent peak corresponds to the  $\text{CH}_3$  terminal methyl symmetric stretch ( $\nu_s$ ) at  $2875\text{ cm}^{-1}$ , with additional peaks corresponding to the  $\text{CH}_2$  symmetric stretch ( $\nu_s$ ) at  $2848\text{ cm}^{-1}$ , the  $\text{CH}_2$  Fermi resonance (FR) at  $2905\text{ cm}^{-1}$ , the  $\text{CH}_3$  FR at  $2938\text{ cm}^{-1}$ , and the  $\text{CH}_3$   $\nu_{as}$  at  $2967\text{ cm}^{-1}$ .<sup>47</sup> Figure 2

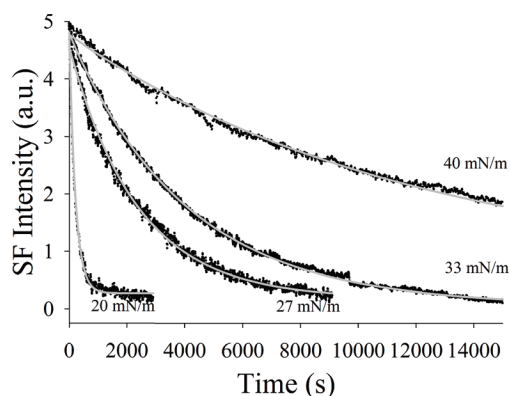


**Figure 3.** Representative decays of the SFVS intensity for the  $\text{CH}_3 \nu_s$  vibration at  $2875 \text{ cm}^{-1}$ . The above decays were collected for DSPC/DSPC- $d_{70}$  bilayers at  $46.8^\circ\text{C}$ . Data are shown in black. Gray lines represent the fit to the data according to eq 13 for deposition pressures of 40, 33, 27, and 20 mN/m.

also shows the spectrum for a DSPC/DSPC- $d_{70}$  bilayer following complete flip-flop (black dash). The SFVS response following flip-flop is identical to that for a symmetrically prepared bilayer with 1:1 DSPC:DSPC- $d_{70}$  in both leaflets (Figure 2, solid black). The spectra are offset for clarity.

Representative decay curves for DSPC flip–flip recorded at  $46.8^\circ\text{C}$  are shown in Figure 3 for pressures of 40 mN/m, 33 mN/m, 27 mN/m, and 20 mN/m. The raw data for each decay are shown in black, with the fit to the data obtained using eq 13 shown as a solid gray line. Table 1 summarizes the rate constant for decay of DSPC/DSPC- $d_{70}$  bilayers as a function of pressure at temperatures of  $40^\circ\text{C}$ ,  $42^\circ\text{C}$ ,  $43^\circ\text{C}$ ,  $46.8^\circ\text{C}$ , and  $50^\circ\text{C}$ . For convenience, the half-life for phospholipid flip-flop is also presented in Table 1. The half-life of decay is related to the rate constant and is given as:<sup>22</sup>

$$t_{(1/2)} = \ln(2)/2k \quad (14)$$

For DSPC bilayers prepared at 30 mN/m, the half-life for lipid flip-flop ranges from greater than 11.5 h to approximately 25 min at  $40.0$  and  $50.0^\circ\text{C}$  respectively. The kinetics also show a large dependence on the lateral membrane pressure, with the half-life for DSPC flip-flop at  $40^\circ\text{C}$  varying from  $\sim 11.5$  h to  $\sim 1$  h for  $\Pi = 30$  mN/m and  $\Pi = 14$  mN/m respectively. Most estimates suggest that the range of monolayer surface pressures which is most representative of physiological membrane bilayers is between 30 and 35 mN/m.<sup>34</sup> Although the pressures studied here are beyond the physiologically relevant range in some cases, the larger pressure range does facilitate more accurate determination of the pressure dependent thermodynamic parameters for flip-flop, including the activation area and work required to reach the transition state.

**Area of Activation for DSPC Flip-Flop.** The kinetic data presented in Table 1 were used to determine the activation area ( $\Delta a^\ddagger$ ) according to the following expression:<sup>36</sup>

$$-RT \left( \frac{\partial \ln(k)}{\partial \Pi} \right)_T = \Delta a^\ddagger \quad (15)$$

As seen in eq 15, the activation energy may be readily determined by plotting  $\ln(k)$  as a function of lateral pressure for a series of decays collected at a single temperature. The data from Table 1 were fit according to eq 15 in order to determine the activation area for DSPC flip-flop at each of the

temperatures studied. The calculated values for  $\Delta a^\ddagger$  were  $57 \pm 7$ ,  $47 \pm 7$ ,  $44 \pm 5$ ,  $40 \pm 5$ , and  $35 \pm 15 \text{ \AA}^2/\text{molecule}$  for  $40.0$ ,  $42.0$ ,  $43.0$ ,  $46.8$ , and  $50.0^\circ\text{C}$ , respectively, and are summarized in Table 2. For comparison, the equilibrium area per molecule for DSPC at 30 mN/m is  $45.9 \pm 1.3 \text{ \AA}^2/\text{molecule}$ , representing the area per molecule occupied for a lipid in a ground state geometry prior to flip-flop ( $a_0$ ). The value of  $45.9 \text{ \AA}^2/\text{molecule}$  for  $a_0$  is obtained from pressure–area isotherms collected during sample deposition. The total area per lipid occupied at the transition state ( $a$ ) (per flip-flop event) is given by

$$a = a_0 + \Delta a^\ddagger \quad (16)$$

For DSPC,  $a$  is calculated from the data in Table 2 to be  $103 \pm 7$ ,  $93 \pm 7$ ,  $90 \pm 5$ ,  $86 \pm 5$ , and  $81 \pm 15 \text{ \AA}^2/\text{molecule}$  at  $40.0$ ,  $42.0$ ,  $43.0$ ,  $46.8$ , and  $50.0^\circ\text{C}$ , respectively. The area per molecule for DSPC in the transition state is nearly double the area per molecule in the ground state. For illustrative purposes, the DSPC molecules in the bilayer can be conceptualized as hexagonally close packed cylinders. Using this model, it is possible to estimate the upper and lower limits for the transition state area, assuming a unimolecular process. For a single lipid molecule in the transition state, the minimum area would be equal to the area of two cylinders plus the excluded area between them, corresponding to a lipid molecule bent back alongside itself (Figure 4A). For DSPC, this lower limit is near  $104 \text{ \AA}^2/\text{molecule}$ . We do not consider torsional or bond angle constraints, as the ground state area for the lipid molecules does not represent a rigid structure, but rather the average area occupied by a lipid which has some limited motional freedom. An upper limit may be estimated from the area of an idealized cylinder turned orthogonal to the surface normal within the bilayer as a rigid rodlike structure (Figure 4B). The transition state area in this case would be approximately  $174 \text{ \AA}^2/\text{molecule}$ , using a value of  $22.75 \text{ \AA}$  for the length of a DSPC molecule in the gel state.<sup>50,51</sup> The agreement between the estimated lower bound and the values for  $a$  measured here is quite good at  $40.0^\circ\text{C}$  and becomes less correlated at higher temperatures. This may be partially due to the assumption of  $a_0 = 45.9 \text{ \AA}^2/\text{molecule}$ , which is only strictly true for monolayers at  $24.0^\circ\text{C}$  and increases slightly ( $\sim 0.1$ – $0.2 \text{ \AA}^2/\text{molecule per }^\circ\text{C}$ ) with increasing temperature.<sup>35,51</sup> Our estimates for the total transition state area are in reasonable agreement with the estimate for the lower bound geometry of a bent lipid structure considering the simple conceptual model employed and the assumption of a hexagonally close packed structure. However, it is important to stress that this idealized estimate is only intended for illustrative purposes and is not necessarily indicative of a unimolecular process for flip-flop. The calculated area of activation does not provide any clues as to the particular configuration of the transition state, the mechanism by which the transition state is reached, or the number of lipids involved in the transition state as  $\Delta a^\ddagger$  is determined on a per-mole basis.

The activation area can also be related to the energetic penalty of adopting a transition state geometry. This is equivalent to the reversible work done by a lipid on the surrounding bilayer in order to reach the transition state. For DSPC/DSPC- $d_{70}$  bilayers at 30 mN/m, the work term,  $\Pi \Delta a^\ddagger$ , is  $10.2 \pm 1.3$ ,  $8.6 \pm 1.3$ ,  $8.0 \pm 0.8$ ,  $7.2 \pm 0.9$ , and  $6.3 \pm 2.6 \text{ kJ/mol}$  for  $40.0$ ,  $42.0$ ,  $43.0$ ,  $46.8$ , and  $50.0^\circ\text{C}$ , respectively. The work required to reach the transition state decreases as the temperature is increased, reflecting the decrease in activation area with increasing temperature. The data indicate that less energy is



**TABLE 1: Kinetics for DSPC Flip-Flop as a Function of Temperature and Lateral Surface Pressure<sup>a</sup>**

$T$ (°C)	$\Pi$ (mN/m)	$\ln(k)$	$t_{(1/2)}$ (min)	$T$ (°C)	$\Pi$ (mN/m)	$\ln(k)$	$t_{(1/2)}$ (min)
40.0	14	-9.36	67.0	42.0	20	-9.03	48.2
	15	-9.06	49.6		22	-9.13	53.5
	16	-9.67	91.5		22	-9.38	68.4
	16	-10.17	151		23	-9.58	83.4
	16	-9.79	103		23	-9.70	94.6
	18	-9.8	104		26	-9.75	98.8
	18	-10.21	156		26	-10.21	157
	20	-10.25	163		28	-9.47	74.9
	20	-10.50	210		28	-9.78	102.2
	22	-10.68	251		28	-10.03	131.3
	23	-10.58	227		30	-10.56	223
	25	-10.32	175		35	-10.75	269
	30	-11.70	696				
43.0	18	-8.81	38.7	46.8	18	-8.43	26.5
	20	-8.46	27.2		20	-8.14	19.8
	20	-8.62	31.9		20	-8.63	32.5
	25	-8.86	40.6		20	-8.91	42.6
	25	-9.00	46.6		23	-8.24	21.9
	26	-8.79	37.9		23	-8.93	43.6
	26	-9.54	80.0		25	-8.36	24.6
	30	-9.39	69.1		25	-8.97	45.6
	30	-9.78	102.1		27	-9.23	58.7
	32	-10.14	146		30	-9.30	62.9
	35	-9.86	111		33	-9.69	93.2
	36	-10.54	218		36	-10.33	176
	26	-10.55	221		40	-10.06	135
	36	-10.54	36				
	36	-10.55	36				
	38	-10.18	38				
	38	-10.54	38				
50.0	24	-8.31	23.5				
	25	-7.70	12.8				
	27	-8.53	29.3				
	30	-8.26	22.3				
	30	-8.62	31.8				
	30	-8.21	21.2				
	33	-8.49	28.0				
	35	-8.49	28.1				
	37	-8.84	39.8				
	38	-9.44	72.7				
	40	-8.68	33.9				

<sup>a</sup> The error in  $\Pi$  is  $\sim \pm 0.2$  mN/m. The error in  $\ln(k)$  and  $t_{(1/2)}$  is  $\pm 2\%$ .

**TABLE 2: Summary of Thermodynamic Data for DSPC Bilayers Prepared at 30 mN/m as a Function of Temperature**

parameter	temperature				
	40.0 °C	42.0 °C	43.0 °C	46.8 °C	50.0 °C
$\Delta a^\ddagger$ (Å <sup>2</sup> /molecule)	$57 \pm 7$	$47 \pm 7$	$44 \pm 5$	$40 \pm 5$	$31 \pm 14$
$\Pi \Delta a^\ddagger$ (kJ/mol)	$10.2 \pm 1.3$	$8.6 \pm 1.3$	$8.0 \pm 0.8$	$7.2 \pm 0.9$	$5.6 \pm 2.5$
$\Delta S^\ddagger$ (J/mol K)	$414 \pm 84$	$408 \pm 84$	$406 \pm 84$	$403 \pm 84$	$399 \pm 85$
$T \Delta S^\ddagger$ (kJ/mol)	$130 \pm 26$	$129 \pm 27$	$128 \pm 27$	$129 \pm 27$	$128 \pm 27$
$\Delta G^\ddagger$ (kJ/mol)	$105 \pm 2$	$105 \pm 2$	$104 \pm 2$	$103 \pm 2$	$102 \pm 2$

required to reach the transition state for flip-flop at an elevated temperature as a result of increased thermal motion and a concomitant relaxing of the packing constraints in the membrane.

As was mentioned above, inclusion of the work term in the activation thermodynamics is essential to an accurate determination of the activation entropy and activation enthalpy. This will be outlined in greater detail in the discussion of the activation enthalpy for DSPC flip-flop below.

**Activation Enthalpy for DSPC Flip-Flop.** The enthalpy of activation for lipid flip-flop is given by

$$\Delta H^\ddagger = E_a + \Pi \Delta a^\ddagger - RT \quad (17)$$

and depends on the Arrhenius activation energy, the temperature, and the work associated with reaching the activated state. The work term is derived from the pressure dependent kinetic data presented above, and the Arrhenius thermodynamic parameters may be determined from the temperature dependence of the rate constant for flip-flop at a fixed pressure. As an example, the kinetics of DSPC flip-flop at 30 mN/m are plotted in Figure 5 as  $\ln(k)$  versus inverse temperature. From the linear-least-squares fit of the data in Figure 5, the values of  $E_a$  and  $A$  for DSPC flip-flop were determined to be  $228 \pm 27$  kJ/mol and  $1.56 \times 10^{33} \text{ s}^{-1} \pm 7 \times 10^{32} \text{ s}^{-1}$ , respectively. The Arrhenius activation energy and pre-exponential factor calculated here are in agree-

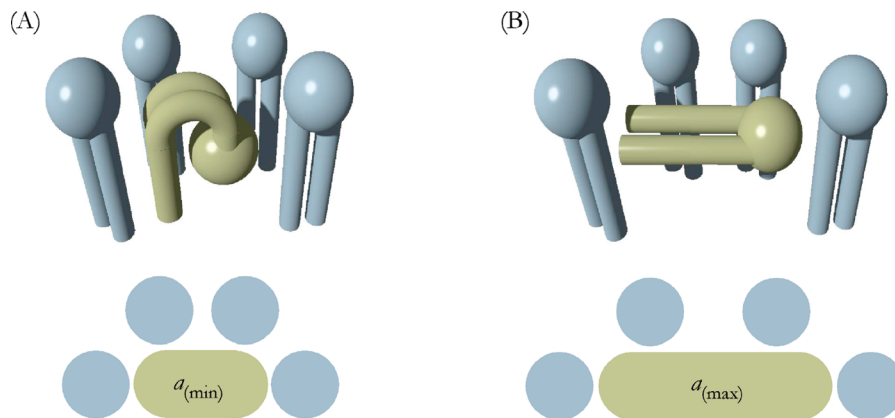


**Figure 4.** Hypothetical minimum (A) and maximum (B) transition state areas corresponding to lipid flip-flop. The minimum area ( $a_{(\min)}$ ) is represented by a lipid bent with the headgroup traversing the bilayer along its chains while only minimally disturbing the surrounding lipids. The estimated area is roughly equal to twice that occupied in a ground state configuration (blue). A hypothetical maximum area ( $a_{(\max)}$ ) would correspond to an extended lipid oriented parallel to the membrane surface (B). This rigid cylinder approximation is a more energetically unfavorable structure, but it provides an estimate of the maximum transition state area possible for a unimolecular flipping mechanism. These illustrations are meant simply as a conceptual tool, as the actual transition state geometry is still unknown.

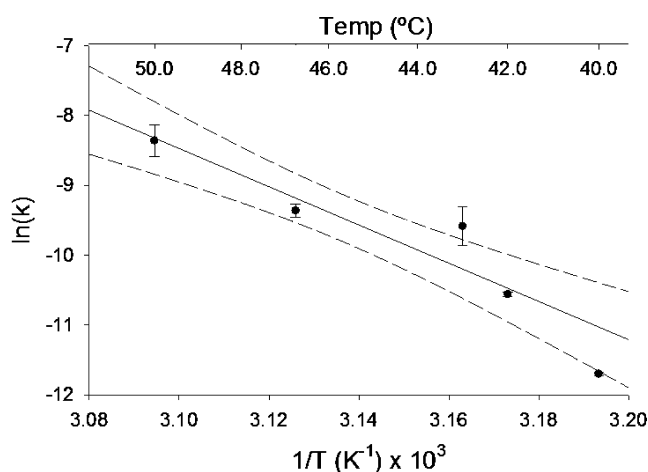


**Figure 5.** Arrhenius plot for DSPC flip-flop at 30 mN/m using the data presented in Table 1. The solid line represents the linear least-squares fit to the data, and the dashed line represents the 95% confidence intervals for the fit.

ment with data previously obtained in our laboratory.<sup>5</sup> The Arrhenius activation energy and work term measured are used to calculate  $\Delta H^\ddagger$ . For DSPC at 30 mN/m,  $\Delta H^\ddagger$  is  $235 \pm 28$ ,  $234 \pm 28$ ,  $233 \pm 28$ ,  $232 \pm 28$ , and  $231 \pm 28$  kJ/mol for lipid flip-flop at 40.0, 42.0, 43.0, 46.8, and 50.0 °C, respectively. The temperature dependence of  $\Delta H^\ddagger$  is due solely to the variation in the work terms at each temperature, as the Arrhenius activation energy is temperature independent. However, care must be taken not to infer any great significance to these differences as the activation enthalpies for DSPC as a function of temperature are not statistically different, given the large error in  $E_a$ . Even with the large uncertainties in  $E_a$ , it is important to note that failure to include the pressure dependent work term leads to an underestimation of the activation enthalpy by approximately 8 kJ/mol. This error is still less than the random error in  $\Delta H^\ddagger$ . However, failure to include the work term introduces *systematic* error in the determination of  $\Delta H^\ddagger$ , reducing the accuracy of the measurement. In addition to the activation enthalpy, we have also determined the activation entropy in order to characterize the relative role each plays in determining the net energy barrier to flip-flop.

**Activation Entropy for DSPC Flip-Flop.** From the thermodynamic data presented in Table 1, it is possible to calculate  $\Delta S^\ddagger$  for lipid flip-flop according to eq 8. For flip-flop of DSPC at 30 mN/m,  $\Delta S^\ddagger$  is found to be  $414 \pm 84$  and  $399 \pm 85$  J/mol K at 40.0 and 50.0 °C, respectively. A summary of  $\Delta S^\ddagger$  values for DSPC flip-flop at all temperatures examined may be found in Table 2. The total energetic contribution of the activation entropy to the lipid flip-flop free energy barrier is given as  $T\Delta S^\ddagger$  and is calculated to be near  $130 \pm 26$  kJ/mol for DSPC at each of the temperatures examined in this study. Specific values for each temperature may be found in Table 2. This large positive value for the entropic term indicates that there is a favorable increase in entropy for a phospholipid moving from the ground state geometry to the transition state. A gel state phospholipid bilayer is a well packed, highly ordered structure with the alkyl chains in a predominantly all-trans structure.<sup>47,52</sup> This ground state arrangement of lipids corresponds to a relatively low entropy system. In the transition state geometry, the polar headgroup must be located in the membrane interior, leading to disturbances in the local packing of the surrounding lipid molecules, decreased order of the lipid undergoing flip-flop, and is likely accompanied by changes in the ordering of water at the interface. The local order of the bilayer and surrounding water is necessarily disturbed by a phospholipid in the transition state, and this is reflected in the large value of  $T\Delta S^\ddagger$ . The pressure dependent term in eq 10 contributes approximately 33 J/mol K to  $\Delta S^\ddagger$  for DSPC at 30 mN/m and 40.0 °C. Inclusion of the pressure dependent terms in the analysis of flip-flop thermodynamics does not in any way affect the total free energy barrier ( $\Delta G^\ddagger$ ) observed. However, evaluation of the work term is essential if any conclusions regarding the enthalpic or entropic components of the free energy barrier are to be made, such as for use in molecular dynamics calculations or as a means of providing insight into the physical nature of the transition state driving lipid translocation, as such variations are not apparent in the analysis of  $\Delta G^\ddagger$  alone.

**Activation Free Energy for DSPC Flip-Flop.** Having determined the activation area and activation entropy for DSPC flip-flop, the net free energy barrier to phospholipid flip-flop can be determined using eq 4. From the values of  $E_a = 228 \pm 28$  kJ/mol,  $RT = 2.6$  kJ/mol,  $\Pi\Delta a^\ddagger = 10.2 \pm 1.3$  kJ/mol, and  $T\Delta S^\ddagger = 130 \pm 26$  kJ/mol,  $\Delta G^\ddagger$  is calculated to be  $105 \pm 2$  kJ/mol at 30 mN/m and 40.0 °C. A summary of the free energy



**TABLE 3: Pressure Dependent Kinetics and Activation Area for DPPC and DMPC**

	$\Pi$ (mN/m)	$T$ (°C)	$k$ (s <sup>-1</sup> ) $\times 10^5$	$t_{1/2}$ (min)		$T$ (°C)	$\Delta a^\ddagger$ (Å <sup>2</sup> /molecule)
DPPC	25	31.0	25.2 $\pm$ 0.4	23 $\pm$ 0.4	DPPC	37.0 <sup>a</sup>	73 $\pm$ 12
	30 <sup>a</sup>	31.0	11.0 $\pm$ 0.6	52 $\pm$ 3		31.0	69 $\pm$ 7
						28.0	114 $\pm$ 7
	25	28.0	20.9 $\pm$ 0.2	27.6 $\pm$ 0.3			
	30 <sup>a</sup>	28.0	5.3 $\pm$ 0.3	109 $\pm$ 6		20.9 <sup>b</sup>	128 $\pm$ 15
DMPC	40	20.9	3.61 $\pm$ 0.01	160.0 $\pm$ 0.4	DMPC	20.9	133 $\pm$ 15
	35	20.9	8.70 $\pm$ 0.01	66.4 $\pm$ 0.1			
	32	20.9	55 $\pm$ 2	10.5 $\pm$ 0.4			

<sup>a</sup> Select kinetic data for DPPC were taken from previous publications.<sup>5</sup> <sup>b</sup> The activation area data for DPPC were extrapolated to 20.9 °C using the measured values in order to facilitate comparison with DMPC.

**TABLE 4: Summary of Flip-Flop Thermodynamics for DSPC, DPPC, and DMPC at 20.9 °C<sup>a</sup>**

	$\Delta G^\ddagger$ (kJ/mol)	$E_a$	$\Delta H^\ddagger$ (kJ/mol)	$T\Delta S^\ddagger$ (kJ/mol)	$\Delta a^\ddagger$ (Å <sup>2</sup> /molecule)	$\Pi\Delta a^\ddagger$ (kJ/mol)
DMPC <sup>b</sup>	84 $\pm$ 1	229 $\pm$ 13	251 $\pm$ 14	167 $\pm$ 12	133 $\pm$ 15	24 $\pm$ 3
DPPC <sup>b</sup>	100.7 $\pm$ 0.3	224 $\pm$ 9	245 $\pm$ 10	143 $\pm$ 8	128 $\pm$ 15	23 $\pm$ 3
DSPC	113 $\pm$ 4	228 $\pm$ 28	243 $\pm$ 29	130 $\pm$ 28	97 $\pm$ 12	18 $\pm$ 2

<sup>a</sup> All temperature dependent values are obtained by extrapolation of the kinetic data to 20.9 °C. The error in the free energy is calculated from the kinetic data, according to eq 2. <sup>b</sup> Thermodynamic data for DPPC and DMPC were calculated using previously published kinetic data.<sup>5,36</sup>

barrier for DSPC flip-flop at each of the temperatures examined is presented in Table 2. The error in  $\Delta G^\ddagger$  is determined from the fit to the kinetic data using eq 2. We observe that the net free energy barrier to phospholipid flip-flop is considerably smaller than the estimate of 228 kJ/mol obtained from  $E_a$ . Inclusion of the activation entropy leads to a significant reduction in the estimated total energy barrier to DSPC flip-flop. It is clear from this analysis that the entropic contributions to flip-flop must be treated in order to obtain an accurate picture of the activation thermodynamics. Knowledge of both the enthalpic and entropic contributions to the thermodynamic barrier should also facilitate modeling of flip-flop for gel phase species and potentially increase our understanding of the mechanism for lipid flipping. By continued application of this method to additional lipid species, it should be possible to catalog the thermodynamic behavior of the many lipid species found in cellular systems. We have undertaken the systematic exploration of flip-flop behavior for different lipid species, beginning with several symmetric phosphocholine (PC) derived lipids of differing acyl chain length, the results of which are presented below.

**Influence of Alkyl Chain Length.** In contrast to the simple DSPC lipid model examined above, cellular membranes consist of a wide variety of lipid components. These lipids vary in the nature of their headgroups, and the saturation and length of their lipid alkyl chains. These differences in structure have important cellular consequences, allowing the membrane to tailor its physical properties based on lipid composition.<sup>53,54</sup> For instance, membrane properties such as permeability, fluidity or lateral mobility, and phase state are linked to alkyl chain structure and composition.<sup>54,55</sup> In order to better understand how the composition of the bilayer influences lipid flip-flop behavior, we have explored the influence of lipid alkyl chain structure on the kinetics and thermodynamics of flipping.

It is possible to examine what influence, if any, the phospholipid alkyl chain length has on the thermodynamic barrier to flip-flop by applying the thermodynamic analysis presented above to the kinetics of flip-flop for shorter chain analogues previously studied in our laboratory. The temperature dependent kinetics and Arrhenius activation thermodynamics for the shorter chain lipids, DPPC and DMPC, have been previously published.<sup>5</sup>

These lipids differ only in the number of carbons (DSPC = 18C, DPPC = 16C, DMPC = 14C) on each of their alkyl chains. In order to compare the transition state thermodynamics of DSPC and DPPC to that for DMPC, it is necessary to extrapolate the data for those species below the gel to liquid phase transition temperature of DMPC ( $T_m$  = 24 °C).<sup>51,56,57</sup> so that the behavior of each of these lipids may be compared in a common phase state ( $T_m$  (DPPC) = 41 °C,  $T_m$  (DSPC) = 55 °C).<sup>58</sup> The kinetic and thermodynamic data for DSPC may be extrapolated to lower temperatures using the data presented above. For DPPC, the pressure dependent thermodynamic parameters, namely, the activation area, have been previously determined but only for a single temperature (37 °C).<sup>36</sup> To facilitate extrapolation to lower temperatures, the pressure dependent kinetics and activation area of DPPC flip-flop were also measured at 28.0 and 31.0 °C, and are presented in Table 3. This data may be used to extrapolate the pressure dependent thermodynamic behavior of DPPC to lower temperatures. The pressure dependent kinetics and activation area for DMPC flip-flop were determined at 20.9 °C, and are reported in Table 3 without extrapolation. The transition state thermodynamics for DSPC were also extrapolated to 20.9 °C, and the thermodynamic data for all three lipid species are summarized in Table 4. The free energy barrier for flip-flop decreases from 113  $\pm$  1 kJ/mol for DSPC to 100.7  $\pm$  0.3 kJ/mol for DPPC and 84  $\pm$  1 kJ/mol for DMPC. Significant increases in  $T\Delta S^\ddagger$  and  $\Pi\Delta a^\ddagger$  are also observed as the chain length decreases. However, the Arrhenius activation energy  $E_a$  is essentially invariant as the chain length is decreased, indicating that the observed decrease in free energy is due to changes in the work and entropy of the transition state versus ground state configurations. This finding suggests that the lipid alkyl chain structure is closely linked to the entropy of the system, while the enthalpy is more closely related to the headgroup chemistry, as DSPC, DPPC, and DMPC all possess the choline functional group.

This observation is consistent with previous studies which suggested that the enthalpic barrier to flip-flop is primarily dependent on headgroup structure.<sup>9,59</sup> The similarity in activation enthalpy for DSPC, DPPC, and DMPC is consistent with the idea that the enthalpic barrier is primarily due to unfavorable interactions between the headgroup and the bilayer core, as these

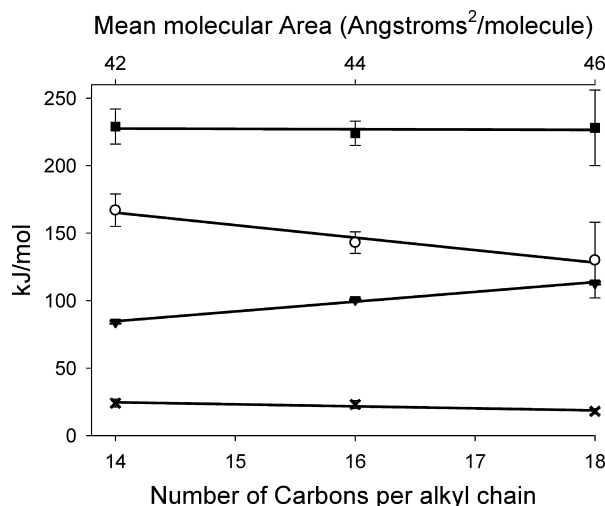


**Figure 6.** Correlation of activation thermodynamics with chain length and mean molecular area. Values of  $E_a$  (■),  $T\Delta S^\ddagger$  (○),  $\Delta G^\ddagger$  (▼), and  $\Pi\Delta a^\ddagger$  (×) are shown for DMPC, DPPC, and DSPC at 20.9 °C as a function of the chain length and membrane packing for each lipid.

interactions have little or no dependence on bilayer thickness. On the other hand, membrane thickness and area per lipid molecule decrease linearly with decreasing chain length. Changes in packing, rather than membrane thickness, would be expected to influence the two-dimensional work term, and changes in either or both of these parameters would be expected to strongly influence the entropic contribution of the activation barrier. For the lipids considered here,  $\Pi\Delta a^\ddagger$  and  $T\Delta S^\ddagger$  decrease linearly with increasing chain length (Figure 6). The increase in  $\Pi\Delta a^\ddagger$  corresponds linearly with the changes in mean molecular area in the films. The shorter chain lipid DMPC is more tightly packed in the ground state ( $a_0 = 42 \pm 1.1 \text{ Å}^2/\text{molecule}$ )<sup>5</sup> than DSPC ( $a_0 = 45.9 \pm 1.3 \text{ Å}^2/\text{molecule}$ ), and more energy is required to accommodate the movement from the ground state to the transition state, which is manifest as a higher work term. Similarly, the larger activation entropy for DMPC is consistent with a more ordered (tightly packed) ground state, assuming that the transition states for DMPC and DSPC are similar. However, the increase in activation entropy with decreasing chain length ( $\Delta(T\Delta S^\ddagger) \sim 6 \text{ kJ/mol per carbon}$ ) is larger than expected based on the changes in the activation area alone ( $\Delta(\Pi\Delta a^\ddagger) \sim 1 \text{ kJ/mol per carbon}$ ; see eq 8), suggesting that the activation entropy is somewhat dependent on membrane thickness as well as lateral packing.

Many of the findings discussed here may be rationalized based only on changes in the ground state configuration of the lipids, such as mean molecular area or membrane thickness. However, the activation parameters may also reflect changes in the transition state configuration as well. If the molar entropy of the transition state remains constant between DPPC and DSPC, the increase in ground state entropy would be manifest as a decrease in the activation entropy. Wimley and Thompson described this possible scenario by the “loss of favorable entropy” when the ground state is more disordered, as is the case for DSPC relative to DPPC.<sup>8</sup> Alternatively, the decrease in activation entropy as chain length is increased may instead be due to increased ordering of the transition state.<sup>8</sup> For DSPC, DPPC, and DMPC, this scenario would suggest an increase of the ordering of the DSPC transition state relative to that of DPPC and DMPC. Based on the calculated  $\Delta a^\ddagger$  values for the three lipids, the total transition state area ( $a$ ) for DSPC ( $143 \pm 12 \text{ Å}^2/\text{molecule}$ ) is slightly smaller than that for DPPC ( $170 \pm 16$

$\text{Å}^2/\text{molecule}$ ) and DMPC ( $175 \pm 15 \text{ Å}^2/\text{molecule}$ ), consistent with the idea that the transition state is more ordered for the longer chained species. It appears that the decreasing trend in the activation entropy with increasing chain length is potentially due to both increasing ground state entropy and decreasing transition state entropy.

**Comparison with Previous Flip-Flop Experiments.** The data obtained herein may be compared with other thermodynamic data for lipid flip-flop found in the literature. Homan and Pownall studied the influence of chain length on flip-flop of fluorescent PC lipid derivatives incorporated at 3% into 1-palmitoyl-2-oleoyl-*sn*-glycero-3-phosphocholine (POPC).<sup>9</sup> For their study, the probe consisted of either *n*-octanoic, *n*-decanoic, or *n*-dodecanoic acid groups in the *sn*-1 position with 9-(1-pyrenyl)nonanoic acid in the *sn*-2 position. The authors noted that the free energy barrier ( $\Delta G^\ddagger = \sim 113 \text{ kJ/mol}$  at 37 °C) consisted of large opposing enthalpic and entropic contributions ( $\sim 154 \text{ kJ/mol}$  and  $138 \text{ J/mol K}$ , respectively), yet were only weakly dependent on the chain length of the probe molecule ( $\sim 1 \text{ kJ/mol per carbon}$ ), when the composition of the lipid matrix was held constant. In contrast, the free energy barrier for flip-flop of the native PC lipids discussed above varied by  $\sim 3.7 \text{ kJ/mol per carbon}$ . It should be noted, however, that, in the study by Homan and Pownall, the probe molecule represented a very minor component of the system, and the similarity in the rate and thermodynamics of flipping for probes of different length may simply reflect the common environment into which they are incorporated. This is contrary to the method used in our work where the local environments, including molecular packing, thickness of the bilayer, and so on, vary from DSPC to DPPC according to the physical structure of each lipid.

Wimley and Thompson examined flip-flop and exchange of radiolabeled [<sup>3</sup>H]DMPC in mixed large unilamellar vesicles of DMPC and DMPE.<sup>8</sup> Transfer of the radiolabeled probe from donor vesicles into acceptor vesicles was characterized over time to determine the combined rates of trans- and intermembrane transfer. They found that flip-flop of pure DMPC in the liquid phase was too rapid to be distinguished from the exchange process, yet estimated the thermodynamic parameters for pure DMPC by extrapolation of the concentration dependence of the mixtures to 0% DMPE. They also observed a large enthalpic contribution ( $\Delta H^\ddagger \sim 117 \text{ kJ/mol}$ ) and an opposing, favorable entropic contribution ( $T\Delta S^\ddagger \sim 26 \text{ kJ/mol}$ ) to the net free energy barrier ( $\Delta G^\ddagger = \sim 95 \text{ kJ/mol}$ ) at 50 °C. The agreement between their results and our own are only qualitative, as the free energy barrier we report for DMPC flip-flop is significantly less (84 kJ/mol), even at much lower temperatures. This discrepancy may reflect the significant differences in methodology for the measurement of flip-flop or may possibly be due to slight differences in the membrane composition between the two methods (the authors incorporated small amounts of a charged lipid species to prevent vesicle aggregation). Yet it is interesting to note that Wimley and Thompson also observed a strong correlation between the activation thermodynamics and the order of the membrane in the ground state as they varied concentration of the DMPE component. The authors also noted that changes in the activation entropy were more important to the overall activation barrier than changes in the activation enthalpy, consistent with the findings presented above for DSPC flip-flop in PSLBs.

Recently, a method for measuring the flip-flop of native lipids in vesicles by small-angle neutron scattering was described.<sup>7</sup> Nakano et al. presented thermodynamic results for the exchange and flip-flop of native DMPC in SUVs at 37.0 °C.<sup>7</sup> They

observed a free energy barrier for flip-flop of  $\Delta G^\ddagger = 104$  kJ/mol, an enthalpic barrier of  $\Delta H^\ddagger = 61.5$  kJ/mol, and an entropic contribution of  $T\Delta S^\ddagger = -42.2$  kJ/mol. Like the other studies reviewed here, the reported free energy barrier for DMPC flip-flop is higher than would be expected based on our findings for DSPC, DPPC, and the extrapolated results for DMPC. However, the enthalpic and entropic contributions to the transition state are at even greater odds with the results reported above due to an unfavorable contribution of the activation entropy to the free energy barrier (negative  $T\Delta S^\ddagger$ ). Intuitively, this seems unlikely, as it would suggest that the activated state is significantly more ordered than the ground state configuration. It is possible that the disagreement is due to the difference in phase state for DSPC (gel) and DMPC (liquid) at the temperatures examined, which will need to be examined further. Additionally, each of the studies mentioned above utilizes methods which require simultaneous measurement of interbilayer exchange and flip-flop, which may introduce some error into the measurement. Lastly, inclusion of the pressure dependence for flip-flop in the calculation of activation thermodynamics yields larger values for both  $\Delta H^\ddagger$  and  $\Delta S^\ddagger$ . Inclusion of the pressure dependence in the literature reviewed above may potentially improve the agreement with the data reported here.

We have also compared the lateral pressure dependent kinetics and thermodynamics of lipid flip-flop measured by Homan and Pownall with our results presented above. In the study by Homan and Pownall, the lipid packing in vesicles was modulated by the application of large external pressures ( $\sim 2$  kbar). The kinetics for flip-flop of the lipid probe OPNPE in POPC decreased by a factor of 4 from 1 bar to 2 kbar.<sup>23</sup> An activation volume ( $\Delta V^\ddagger$ ), rather than an activation area, was determined from the dependence of the rate on applied pressure and was calculated to be  $\Delta V^\ddagger = 17 \pm 2$  mL/mol at 50 °C. The authors attributed the decrease in kinetics with applied pressure to an increase in the in-plane packing of the lipids over the pressure range examined, consistent with our findings presented above.<sup>23</sup> Assuming that the local membrane thickness does not change significantly over the range of pressures examined, an equivalent activation area of only  $\sim 2$  Å<sup>2</sup>/molecule is calculated for flip-flop of OPNPE in POPC using a value of 25.8 Å for the thickness of a POPC bilayer.<sup>60</sup> Although this value is small, it is quite consistent with the trends we observe for activation area as a function of packing density. The average area per POPC ( $\sim 65$  Å<sup>2</sup>/molecule)<sup>61</sup> is significantly larger than that for the PC lipids studied here (42–46 Å<sup>2</sup>/molecule), and given the decreasing trend in activation area with area per molecule which we observed the activation area should be quite small. The small calculated activation area may also reflect the different phase states of the POPC membranes (liquid) relative to the gel phase membranes used in our study. Nonetheless, both our findings and those of Homan and Pownall indicate that a local expansion of the membrane is required to accommodate transmembrane movement of a lipid species. Such local expansion may be the result of transient fluctuations and formation of transient defects which are dependent on the local packing of the membrane.<sup>9,23</sup>

Several recent computational studies have calculated the thermodynamic barrier to lipid transmembrane diffusion<sup>62</sup> and the rate of lipid migration through chemically induced transmembrane pores<sup>21</sup> for a series of similar phospholipids. In the first of these studies, atomistic molecular dynamics simulations were used to calculate potentials of mean force describing the free energy barrier to moving a lipid from the membrane exterior to the membrane core. This is accomplished by determining the energy difference between the lamellar system and one in

which two of the lipid molecules are pulled into the bilayer center. The authors found a similar trend of an increasing energy barrier with increasing chain length, although the magnitude of the calculated energy barriers ( $\Delta G^\ddagger = 40$  kJ/mol for DMPC and  $\Delta G^\ddagger = 80$  kJ/mol for DPPC) are lower than those we measured, due in part to the higher temperatures used in the simulation (323 K). The authors also noted a slight mismatch between the calculated and experimental molecular areas, which may somewhat alter the observed free energy barriers. Nonetheless, the trends in the calculated energy barriers with chain length and area are consistent with our own findings. The rates of flip-flop for several different lipid species have also been calculated in atomistic scale calculations wherein a chemically induced water pore is formed by localizing a polar molecule within the bilayer core.<sup>21</sup> This perturbation facilitates computational modeling by increasing the probability of observing a flip-flop event through the preformed pore. The calculated rate of flip-flop through the chemically induced pore shows a significant dependence on alkyl chain length for related phosphocholine lipid species (DMPC and DPPC at 323 K). The total number of lipids diffusing through the pore per unit time also decreases with increasing chain length while the transit time increases.<sup>21</sup> The mechanisms of the pore-mediated flip-flop and the spontaneous flip-flop in single component bilayers may differ significantly, yet in both of these cases a similar dependence of the flip-flop rate on the lipid alkyl chain structure was calculated, consistent with the experimental observations made by SFVS.

## Conclusions

We have determined the influence of lateral pressure and lipid packing density on the flip-flop of native phospholipid species in PSLBs. Increasing lateral pressure is found to significantly limit the kinetics of transmembrane diffusion. The activation thermodynamics for flip-flop of DSPC, DPPC, and DMPC were explored as a function of temperature and pressure in order to determine the influence of alkyl chain length on the energetic barrier to flip-flop. For each of the species examined,  $\Delta G^\ddagger$  consists of a large opposing contributions from  $\Delta H^\ddagger$  and  $\Delta S^\ddagger$ . An increase in alkyl chain length is found to have little influence on  $\Delta H^\ddagger$ . In fact, the only variation in  $\Delta H^\ddagger$  among the three lipid species studied can be attributed to the slight differences in  $\Pi\Delta a^\ddagger$  that accompany changes in membrane thickness and lipid packing. On the other hand,  $\Delta S^\ddagger$  decreases linearly with increasing chain length and is primarily responsible for the chain length dependence of the net energy barrier  $\Delta G^\ddagger$ . Our data suggest that membrane packing, and to some extent membrane thickness, alter the energetic barrier to flip-flop by altering the entropy of the ground and transition state configurations. This is consistent with the idea that the activation enthalpy depends on the nature of the headgroup, which is conserved among these lipid species, and that the entropic contribution reflects the degree of order in the membrane. Additional studies to examine the influence of the headgroup chemistry are underway to address this possibility.<sup>63</sup>

Although there is good qualitative agreement between the thermodynamic trends presented here and those found in the literature for lipid flip-flop, it is important to note how key differences in methodologies may affect the observed values and possibly explain the quantitative differences between studies. It has been demonstrated that DMPC exhibits more rapid flip-flop than its longer chain analogues, such as DPPC and DSPC, and will therefore have a correspondingly smaller free energy barrier to flip-flop.<sup>5</sup> However, the free energy barrier for DMPC flip-flop has been reported in two cases to be greater than or



comparable to that presented here for the longer chain DSPC.<sup>7,8</sup> The larger of the two reported values utilizes a fluorescently labeled lipid probe molecule. It has been previously demonstrated that the use of bulk fluorescent labels leads to hindered flip-flop relative to the native species.<sup>5</sup> In addition, both of the previous studies rely on intervesicle exchange from small unilamellar vesicles (SUVs) to acceptor vesicles in solution. The use of SUVs presents another complication, and lipid flip-flop in SUVs also been shown to exhibit altered flip-flop kinetics relative to less strained systems such as large unilamellar vesicles (LUVs).<sup>37</sup> Lastly, the phase state of the membranes must be considered when comparing two model systems. Flip-flop kinetics in PSLBs are determined for lipids in the gel state, as flip-flop becomes too rapid for accurate measurement by SFVS as the phase transition temperature is approached. The literature sources reviewed here rely instead on liquid crystalline phase membranes, as this is thought to be more representative of biological membranes. It has been observed that flip-flop is more rapid above the phase transition temperature than below, but it is not entirely clear how the interplay of labeling, membrane curvature, and phase state ultimately alters the observed kinetics.<sup>10</sup>

The ability to control lateral pressure and packing of the membrane lipids by LB/LS deposition allows simple determination of the pressure dependent thermodynamic parameters. Although it is possible to make such measurements by application of large external pressures to liposome solutions, the two-dimensional approach has the advantage of simple interpretation (no need to deconvolute bilayer thickness and packing density) and ease of application.

It is also worth noting that the thermodynamic parameters presented herein are derived on a *per mol* basis and do not in any way indicate the absolute geometry or number of molecules involved in the transition state for phospholipid flip-flop. Ensemble thermodynamic parameters determined in this way describe the average behavior of the system and are not indicative of the behavior of a single lipid molecule. Nonetheless, they provide an essential component in our understanding of the driving forces and energetic barriers found in the ensemble system. This method of analysis may be readily applied to other membrane systems in order to examine the effects of additional membrane components on the thermodynamics of flip-flop. In addition to expanding our understanding of the process of flip-flop, it is our hope that such thermodynamic analysis may provide a new perspective into the energetic consequences of generating and maintaining cell membrane asymmetry.

**Acknowledgment.** This work was supported by funds from the National Science Foundation (NSF 0808923 and NSF 0515940). Any opinions, findings, conclusions, or recommendations expressed in this material are those of the authors and do not necessarily reflect the views of the NSF.

## References and Notes

- (1) Kol, M. A.; de Kruijff, B.; de Kroon, A. I. P. M. *Semin. Cell Dev. Biol.* **2002**, *13*, 163.
- (2) Raggars, R. J.; Pomorski, T.; Holthuis, J. C. M.; Kalin, N.; Van Meer, G. *Traffic* **2000**, *1*, 226.
- (3) Roseman, M. A.; Thompson, T. E. *Biochemistry* **1980**, *19*, 439.
- (4) Roseman, M.; Litman, B. J.; Thompson, T. E. *Biochemistry* **1975**, *14*, 4826.
- (5) Liu, J.; Conboy, J. C. *Biophys. J.* **2005**, *89*, 2522.
- (6) Kornberg, R. D.; McConnell, H. M. *Biochemistry* **1971**, *10*, 1111.
- (7) Nakano, M.; Fukuda, M.; Kudo, T.; Endo, H.; Handa, T. *Phys. Rev. Lett.* **2007**, *98*, 238101.
- (8) Wimley, W. C.; Thompson, T. E. *Biochemistry* **1991**, *30*, 1702.
- (9) Homan, R.; Pownall, H. J. *Biochim. Biophys. Acta* **1988**, *938*, 155.
- (10) John, K.; Schreiber, S.; Kubelt, J.; Herrmann, A.; Muller, P. *Biophys. J.* **2002**, *83*, 3315.
- (11) Adayev, T.; Estephan, R.; Meserole, S.; Mazza, B.; Yurkow, E.; Banerjee, P. J. *Neurochem.* **1998**, *71*, 1854.
- (12) Contreras, F. X.; Basanez, G.; Alonso, A.; Herrmann, A.; Goni, F. M. *Biophys. J.* **2005**, *88*, 348.
- (13) Steen, A. T. M. V. D.; Jong, W. A. C. D.; Kruijff, B. D.; Deenen, L. L. M. V. *Biochim. Biophys. Acta* **1981**, *647*, 63.
- (14) Cabral, D. J.; Small, D. M.; Lilly, H. S.; Hamilton, J. A. *Biochemistry* **1987**, *26*, 1801.
- (15) Buton, X.; Morrot, G.; Fellmann, P.; Seigneuret, M. *J. Biol. Chem.* **1996**, *271*, 6651.
- (16) Gummadi, S. N.; Menon, A. K. J. *Biol. Chem.* **2002**, *277*, 25337.
- (17) Gurtovenko, A. A.; Vattulainen, I. J. *Phys. Chem. B* **2007**, *111*, 13554.
- (18) Marti, J.; Csajka, F. S. *Europhys. Lett.* **2003**, *61*, 409.
- (19) Marti, J.; Csajka, F. S. *Phys. Rev. E* **2004**, *69*, 1.
- (20) Tieleman, D. P.; Marrink, S.-J. *J. Am. Chem. Soc.* **2006**, *128*, 12462.
- (21) Gurtovenko, A. A.; Onike, O. I.; Anwar, J. *Langmuir* **2008**, *24*, 9656.
- (22) Liu, J.; Conboy, J. C. *J. Am. Chem. Soc.* **2004**, *126*, 8376.
- (23) Homan, R.; Pownall, H. J. *J. Am. Chem. Soc.* **1987**, *109*, 4759.
- (24) Devaux, P. F.; Fellmann, P.; Herve, P. *Chem. Phys. Lipids* **2002**, *116*, 115.
- (25) McIntyre, J. C.; Sleight, R. G. *Biochemistry* **1991**, *30*, 11819.
- (26) Bishop, D. G.; Kamp, J. A. F. O. D.; Deenen, L. L. M. V. *Eur. J. Biochem.* **1977**, *80*, 381.
- (27) Devaux, P. F.; Zachowski, A. *Chem. Phys. Lipids* **1994**, *73*, 107.
- (28) Anglin, T. C.; Liu, J.; Conboy, J. C. *Biophys. J.* **2007**, *92*, L01.
- (29) Laskin, J.; Futrell, J. H. J. *Phys. Chem. A* **2003**, *107*, 5836.
- (30) Steinfeld, J. I.; Francisco, J. S.; Hase, W. L. *Chemical Kinetics and Dynamics*, 2nd ed.; Prentice-Hall: Englewood, NJ, 1998.
- (31) Houston, P. L. *Chemical Kinetics and Reaction Dynamics*; Dover: Mineol, 2001.
- (32) Eyring, H. *Chem. Rev.* **1935**, *17*, 65.
- (33) Wynne-Jones, W. F. K.; Eyring, H. J. *Chem. Phys.* **1935**, *3*, 492.
- (34) Marsh, D. *Biochim. Biophys. Acta, Biomembr.* **1996**, *1286*, 183.
- (35) Cevc, G.; Marsh, D. *Phospholipid Bilayers, Physical Principles and Models*; John Wiley and Sons: New York, 1987.
- (36) Anglin, T. C.; Conboy, J. C. *Biophys. J.* **2008**, *95*, 186.
- (37) Wimley, W. C.; Thompson, T. E. *Biochemistry* **1990**, *29*, 1296.
- (38) Langmuir, I. *J. Chem. Phys.* **1933**, *1*, 756.
- (39) Langmuir, I. *Science* **1936**, *84*, 379.
- (40) Kim, G.; Gurau, M. C.; Lim, S.-M.; Cremer, P. S. *J. Phys. Chem. B* **2003**, *107*, 1403.
- (41) Liu, J.; Conboy, J. C. *J. Am. Chem. Soc.* **2004**, *126*, 8894.
- (42) Liu, J.; Conboy, J. C. *J. Phys. Chem. C* **2007**, *111*, 8988.
- (43) Chen, X.; Wang, J.; Boughton, A. P.; Kristalyn, C. B.; Chen, Z. *J. Am. Chem. Soc.* **2007**, *129*, 1420.
- (44) Chen, X.; Wang, J.; Kristalyn, C. B.; Chen, Z. *Biophys. J.* **2007**, *93*, 866.
- (45) Shen, Y. R. *The Principles of Nonlinear Optics*; John Wiley and Sons, Inc.: New York, 1984.
- (46) Miranda, P. B.; Shen, Y. R. *J. Phys. Chem. B* **1999**, *103*, 3292.
- (47) Liu, J.; Conboy, J. C. *Langmuir* **2005**, *21*, 9091.
- (48) Dick, B.; Gierulski, A.; Marowsky, G.; Reider, G. A. *Appl. Phys. B: Laser Opt.* **1985**, *B35*, 107.
- (49) Guyot-Sionnest, P.; Shen, Y. R.; Heinz, T. F. *Appl. Phys. B: Lasers Opt.* **1987**, *42*, 237.
- (50) Lis, L. J.; McAlister, M.; Fuller, N.; Rand, R. P. *Biophys. J.* **1982**, *37*, 657.
- (51) Marsh, D. *CRC Handbook of Lipid Bilayers*; CRC Press: Boca Raton, FL, 1990.
- (52) Mendelsohn, R.; Davies, M. A.; Brauner, J. W.; Schuster, H. F.; Dluhy, R. A. *Biochemistry* **1989**, *28*, 8934.
- (53) Meer, G. v.; Voelker, D. R.; Feigenson, G. W. *Nat. Rev. Mol. Cell Biol.* **2008**, *9*, 112.
- (54) Baldassare, J. J.; Rhinehart, K. B.; Silbert, D. F. *Biochemistry* **1976**, *15*, 2986.
- (55) Chiang, Y.-W.; Shimoyama, Y.; Feigenson, G. W.; Freed, J. H. *Biophys. J.* **2004**, *87*, 2483.
- (56) Fox, C. B.; Myers, G. A.; Harris, J. M. *Appl. Spectrosc.* **2007**, *61*, 465.
- (57) Lewis, R. N. A. H.; Zhang, Y.-P.; McElhaney, R. N. *Biochim. Biophys. Acta* **2005**, *1668*, 203.
- (58) Koynova, R.; Caffrey, M. *Biochim. Biophys. Acta* **1998**, *1376*, 91.
- (59) Kol, M. A.; van Laak, A. N. C.; Rijkers, D. T. S.; Killian, J. A.; de Kroon, A. I. P. M.; de Kruijff, B. *Biochemistry* **2003**, *42*, 231.
- (60) Nezil, F. A.; Bloom, M. *Biophys. J.* **1992**, *61*, 1176.
- (61) Koenig, B. W.; Dietrich, U.; Klose, G. *Langmuir* **1997**, *13*, 525.
- (62) Sapay, N.; Bennett, W. F. D.; Tieleman, D. P. *Soft Matter* **2009**, *5*, 3295.
- (63) Anglin, T. C.; Conboy, J. C. *Biochemistry* **2008**, *48*, 10220.